

LCC	-----MDGVLWRVRTAALMAALLALAAWALVWASPSVEAQSNPYQRGPNPTRSALTADGPFPSVA-	59
TFC	<u>MAVMTPRRERSLLSRALQVTAATAALVTAVSLAAPAHAAANPYERGNPTDALLEASSGPFVS</u>	65
SEL	-----AANPYERGPAPTNASIEASRGPYATS	26
LCC	TYTVSRLSVSGFGGGVIYYPTG-TSLTFGGIAMSPGYTADASSLAWLGRRLASHGFVVLVINTNS	123
TFC	EENVSRLSASGFGGGTIYYPR--ENNTYGAVAI SPGYTGTEASIAWLGERIASHGFFVITIDTIT	128
SEL	QTSVSSLVASGFGGGTIYYPTSTADGTFGAVVISPGFTAYQSSIAWLGPRLASQGFVVFTIDTNT	91
LCC	RFDYPDSRASQLSAALNYLRTSSPSAVRARLDANRLAVAGHSMGGGGTLRIAEQNPSLKAAPVPLT	188
TFC	TLDQPDSRAEQLNAALNHMINRASSTVRSRIDSSRLAVMGHSMGGGGTLRLASQRPDLKAAIPLT	193
SEL	TLDQPDSRGRQLLSALDYLTQRSS--VRTRVDATRLGVMGHSMGGGSLEAAKSRTSLKAAIPLT	154
LCC	PWHTDKTFNTS-VPVLIVGAEADTVAPVSQHAIPFYQNLPSSTTPKVYVELDNASHFAPNSNNAI	252
TFC	PWHLNKNWSSVTVPPLIIIGADLDTIAPVATHAKPFYNSLPSSISKAYLELDGATHFAPNIPNKII	258
SEL	GWNTDKTWPELRTPTLVVGADGDTVAPVATHSKPFYESLPGSLDKAYLELRGASHFTPNTSDTTI	219
LCC	SVYTISWMKLWVDNDTRYRQFLCNVNDPALSDFRTNNRHCQ	293
TFC	GKYSVAWLKRFVDNDTRYTQFLCPGPRDGLFGEVEEYRSTCPF	301
SEL	AKYSISWLKRFIDSTRYEQFLCPIPRPSLT--IAEYRGTCPHTS	262

Fig. S1. Sulaiman *et al.*

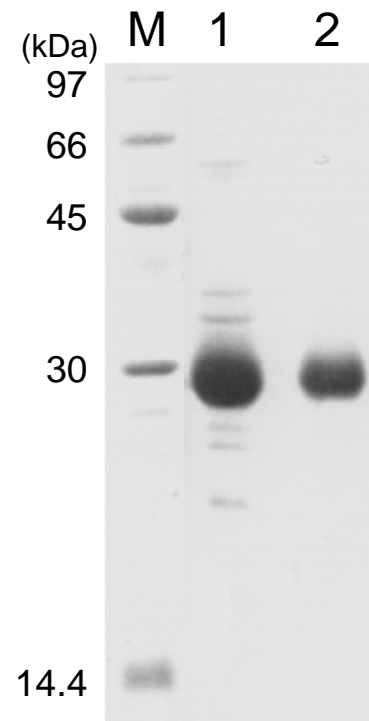


Fig. S2. Sulaiman *et al.*

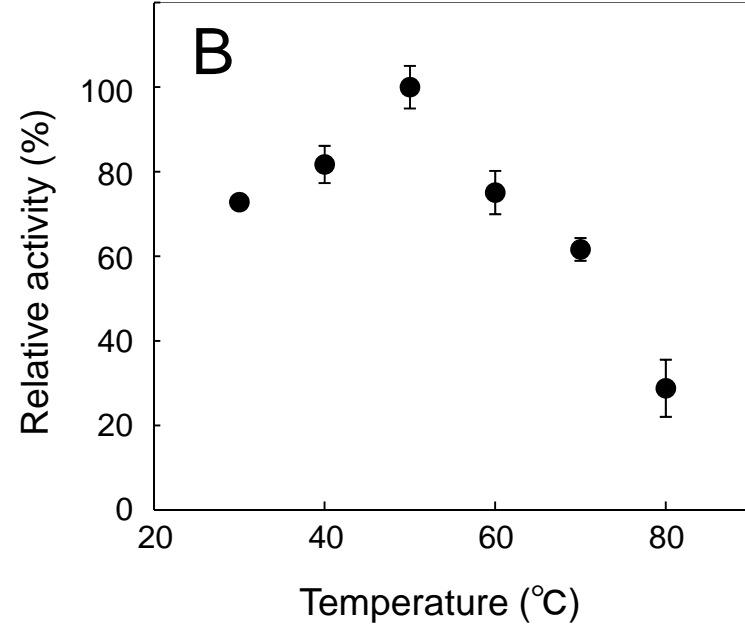
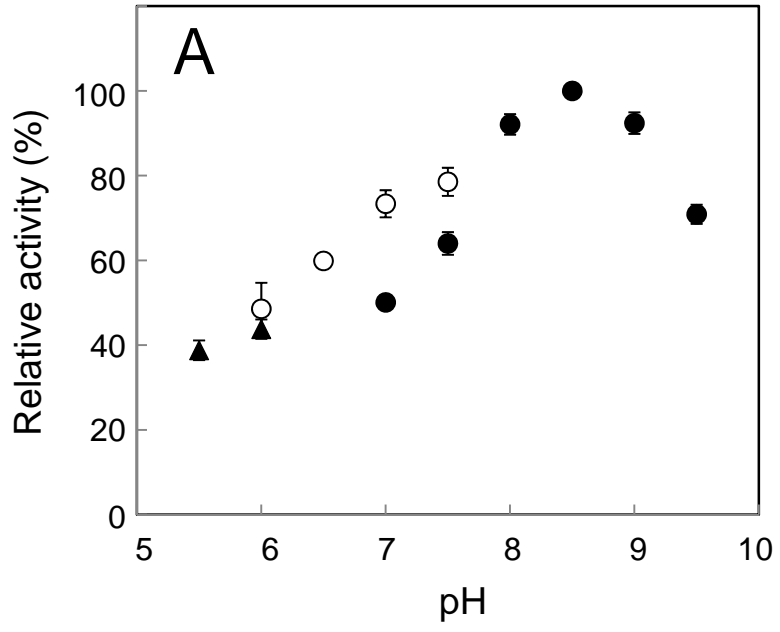


Fig. S3. Sulaiman *et al.*

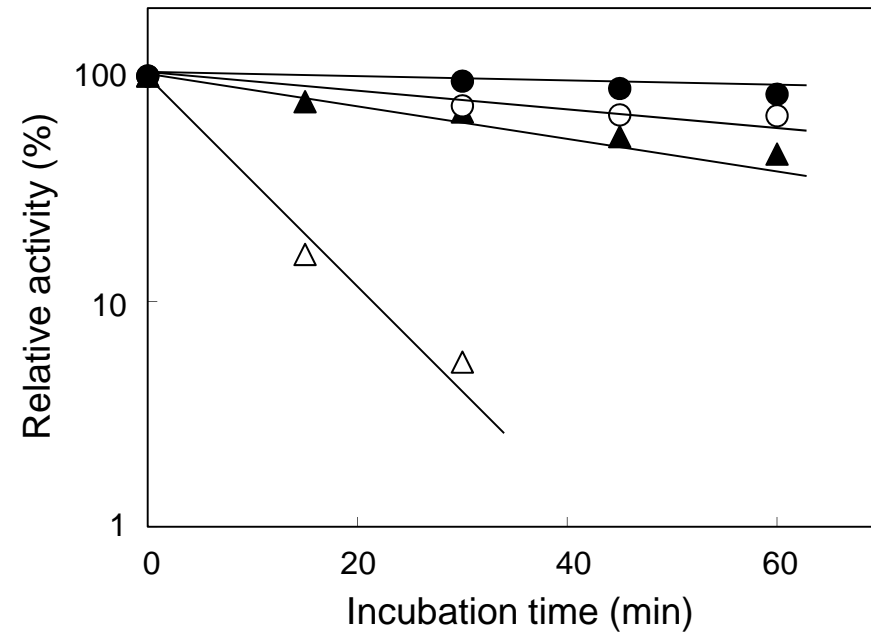


Fig. S4. Sulaiman *et al.*

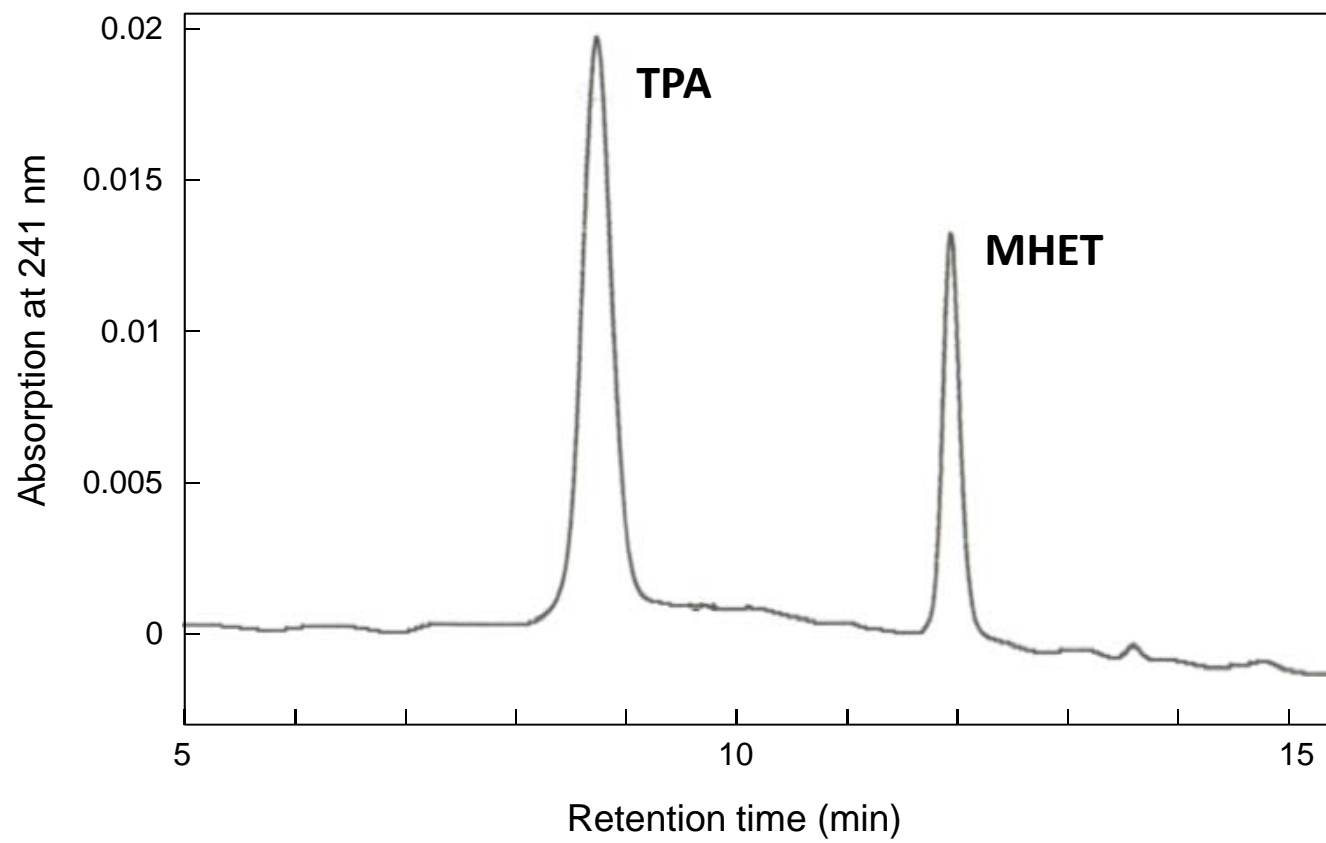


Fig. S5. Sulaiman *et al.*

Figure legends

Figure S1. *Alignment of the amino acid sequences of LC-cutinase (LCC), T. fusca cutinase (TFC), and S. exfoliates lipase (SEL). Gaps are denoted by dashes. The amino acid residues that form a catalytic triad and an oxyanion hole are denoted by solid and open circles, respectively. A pentapeptide GxSxG sequence motif containing the active-site serine residue is boxed. The signal sequences are underlined. It is experimentally determined for TFC (ref. 1) or is estimated for LCC using SMART (<http://smart.embl.de>). The numbers represent the positions of the amino acid residues starting from the N terminus of the protein (the protein without signal peptide for SEL). The accession numbers of TFC and SEL are YP_288944 and 1JFR_A, respectively.*

Figure S2. *Comparison of the purity of LC-cutinase* by SDS-PAGE. Samples were subjected to electrophoresis on a 12% polyacrylamide gel in the presence of SDS. After electrophoresis, the gel was stained with Coomassie brilliant blue. M, low-molecular-weight marker kit (GE Healthcare); lane 1, fraction after SP-Sepharose column chromatography; lane 2, purified LC-cutinase*.*

Figure S3. *pH and temperature dependencies of LC-cutinase*. (A) pH dependency of LC-cutinase*. The enzymatic activity was determined at 30°C using pNP-butyrate as a substrate in 10 mM sodium acetate (pH 5.5, 6.0) (solid triangle), 10 mM sodium phosphate (pH 6.0-7.5) (open circle), or 10 mM Tris-HCl (pH 7.0-9.5) (solid circle) containing 2% acetonitrile. The activity relative to that determined at pH 8.5 is shown as a function of pH. (B) Temperature dependency of LC-cutinase*. The enzymatic*

activity was determined in 10 mM sodium phosphate (pH 7.0) containing 2% acetonitrile at various temperatures using *p*NP-butyrates as a substrate. The activity relative to that determined at 50°C is shown as a function of temperature. The experiment was carried out at least twice and the average values are shown together with error bars.

Figure S4. Stability of LC-cutinase* against irreversible heat inactivation. Semilog plots of the residual activity *versus* the incubation time are shown. LC-cutinase* was incubated in 10 mM sodium phosphate (pH 7.0) at 50°C (solid circle), 60°C (open circle), 70°C (solid triangle), or 80°C (open triangle). Aliquots of each sample were withdrawn at the times indicated and the enzymatic activity was determined at 30°C using *p*NP-butyrates as a substrate. The line was obtained by linear regression of the data.

Figure S5. Separation of degradation products of PET with LC-cutinase* on reverse-phase HPLC. An aliquot of the degradation products of a PET film with LC-cutinase* was directly loaded on a Cosmosil 5C₁₈-AR-II column (4.6 x 250 mm, Nacalai Tesque Inc, Kyoto, Japan) equilibrated with 10% (v/v) solvent B in solvent A. Elution was performed by raising linearly the concentration of solvent B in solvent A from 10 to 40% (v/v) over 15 min. Solvent A was aq. 0.25% (v/v) trifluoroacetic acid and solvent B was acetonitrile. The flow rate was 1.0 ml/min. The degradation products of PET were detected by a UV detector set at 241 nm, at which terephthalic acid (TPA) and its esters exhibit the highest absorption coefficient (ref. 2). TPA and mono (2-hydroxyethyl) terephthalate (MHET) were eluted from the column with the retention

times of 9.1 and 12.3 min, respectively, both of which were identical with those of TPA commercially available (Tokyo Chemical Industry Co. Ltd., Tokyo, Japan) and MHET produced from bis (2-hydroxyethyl) terephthalate (BHET) (Tokyo Chemical Industry Co. Ltd., Tokyo, Japan) upon partial hydrolysis (ref. 3).

References

1. **Chen, S., X. Tong, R. W. Woodard, G. Du, J. Wu, and J. Chen.** 2008. Identification and characterization of bacterial cutinase, *J. Biol. Chem.* **283**:25854–25862.
2. **Yoon, M. Y., J. Kellis, and A. J. Poulouse.** 2002. Enzymatic modification of polyester. *AATCC Rev.* **2**:33-36.
3. **Vertommen, M. A. M. E., V. A. Nierstrasz, M. van der Veer, and M. M. C. G. Warmoeskerken.** 2005. Enzymatic surface modification of poly(ethylene terephthalate). *J. Biotechnol.* **120**:376-386.